

## Efficient single particle detection with a superconducting nanowire

Hatim Azzouz,<sup>1,2</sup> Sander N. Dorenbos,<sup>2</sup> Daniel De Vries,<sup>3</sup> Esteban Bermúdez Ureña,<sup>2</sup> and Valery Zwiller<sup>2</sup>

<sup>1</sup>Physics Department, Stockholm University, SE 106 91 Stockholm, Sweden

<sup>2</sup>Kavli Institute of Nanoscience, Delft University of Technology, P.O. Box 5046, 2600 GA Delft, The Netherlands

<sup>3</sup>Radiation and Isotopes for Health, Delft University of Technology, Mekelweg 15, 2629 JB Delft, The Netherlands

(Received 8 February 2012; accepted 16 July 2012; published online 24 July 2012)

Detection of  $\alpha$ - and  $\beta$ -particles is of paramount importance in a wide range of applications. Current particle detectors are all macroscopic and have limited time resolution. We demonstrate a nanoscale particle detector with a small detection volume, high detection efficiency, short dead times and low dark count levels. We measure  $\alpha$ - and  $\beta$ -particle detection efficiencies close to unity using different sources and also demonstrate blindness towards  $\gamma$ -rays. Our nanoscale detector offers particle detection measurements with unprecedented spatial resolution. *Copyright 2012 Author(s). This article is distributed under a Creative Commons Attribution 3.0 Unported License.* [<http://dx.doi.org/10.1063/1.4740074>]

Since the first detection of  $\beta$ -particles with photographic films by Becquerel,<sup>1</sup> detectors with higher efficiency, lower noise level, higher time resolution, better energy resolution and higher saturation rates have been developed.<sup>2</sup> Scintillation<sup>3</sup> and semiconductor counters<sup>4</sup> provide high detection efficiencies albeit with large detection volumes. Micro-calorimeters based on superconducting transition edge sensors are currently among the smallest particle detectors with absorber dimensions as small as  $(400 \times 400 \times 250) \mu\text{m}$ ,<sup>5</sup> still far from the nanoscale. The readout time of these devices is of the order of milliseconds, limiting the detection rate to  $\sim 100$  Hz. Additionally, low operating temperatures<sup>6</sup> on the order of 100 mK further reduce their applicability.

It has been shown that superconducting nanowires can detect single photons<sup>7</sup> and single electrons.<sup>8</sup> Here we extend this concept to the detection of high energy particles and experimentally demonstrate an efficient nanowire-based device for single  $\alpha$ - and  $\beta$ -particle detection fabricated using standard nanofabrication techniques.<sup>9</sup> Our superconducting nanowire particle detector (SNPD) is a  $500 \mu\text{m}$  long NbTiN nanowire, 100 nm wide and 5 nm thick meandering over a  $10 \mu\text{m}$  diameter disk with a fill factor of 50%, as shown in figure 1. The device is operated at 4.2 K, well below the superconducting transition ( $T_c \sim 12$  K) and biased with a constant dc current ( $I_b$ ) slightly below the critical current ( $I_c$ ).<sup>10</sup> An incident particle can release enough energy in the nanowire to form a hotspot, where superconductivity is destroyed.<sup>10</sup> If the detector wire is sufficiently narrow compared to the hotspot, the increased current density eventually exceeds the critical current density, resulting in a resistive region causing a voltage spike that is then amplified and counted.<sup>7</sup> In the final phase, the hotspot cools down through electron-phonon scattering and the superconducting state is restored within nanoseconds. The detection pulse decay is determined by the kinetic inductance  $L_k$  and the load impedance  $R_A = 50 \Omega$ , and is given by  $\tau = L_k/50 \Omega$ . For the devices used in our work, the decay time  $\tau$  was measured to be in the order of 5 ns, yielding a saturation count rate of 200 MHz and a kinetic inductance  $L_k \sim 250$  nH. The detection time jitter of these detectors has been measured to be better than 60 ps with pulsed laser excitation.<sup>11</sup>

Figure 1 shows a schematic of the experimental setup. The scanning electron microscope (SEM) images of the device reveal the meandering NbTiN nanowire. Each detection event generates a pulse (with  $\sim 2$  mV amplitude after  $\sim 54$  dB amplification) as shown in the inset of figure 1. We successively



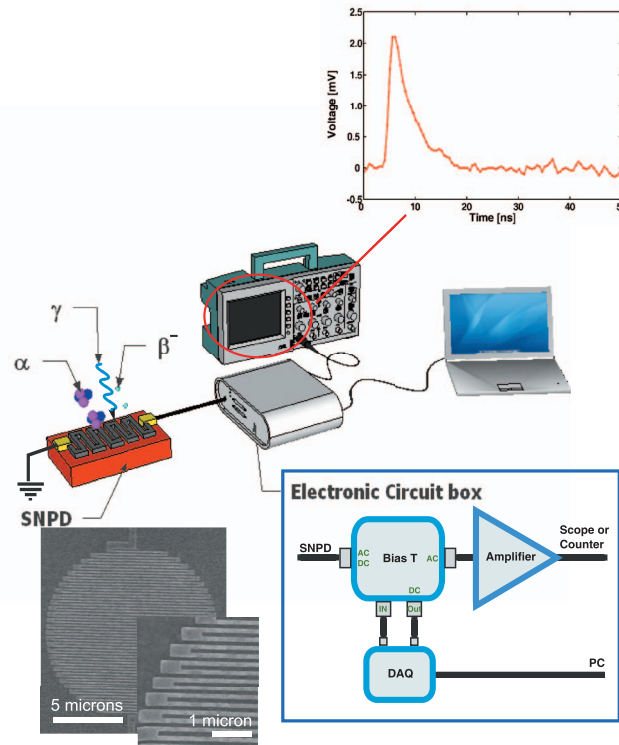


FIG. 1. Schematic layout. Impinging  $\alpha$ -,  $\beta$ - and  $\gamma$ -particles on the detector. The SEM image shows the meandering superconducting nanowire detector. The pulse is a representative detection pulse. For a more detailed description of the electronics box see Supplemental Material.<sup>12</sup>

TABLE I. Detection efficiency comparison. Measured and published data for a wide range of particle energies. The  $\alpha$ -emitting radionuclide  $^{241}\text{Am}$  decay is accompanied by significant amounts of the relevant X- and  $\gamma$ -ray emissions. These include X- and  $\gamma$ -ray emissions probabilities totalling no less than  $\sim 37\%$  and  $38\%$ , respectively.<sup>13</sup>

Source	Type	Initial Activity	Average Energy	Published Half-life ( $t_{1/2}$ )	Detection Efficiency (DE)	Reference for DE
$^{210}\text{Po}$	$\alpha$	41.2 kBq	5.30 MeV	138.38 days	$0.78 \pm 0.18$	Present work
$^{42}\text{K}$	$\beta^-$	40 MBq	3.52 MeV	12.36 hours	$0.95 \pm 0.14$	Present work
$^{31}\text{Si}$	$\beta^-$	26 MBq	1.49 MeV	2.62 hours	$1.06 \pm 0.12$	Present work
$^{241}\text{Am}$	$\gamma, X$	—	$\sim 5.95$ keV	—	$0 \pm 0.10$	Present work
SEM	$e^-$	—	10 keV	—	$\sim 1$	8
Laser	$h\nu$ (photon)	—	$\sim 1$ keV	—	$0.2 @ 1.3$ nm	9

tested our detector with a pure  $\alpha$ -source ( $^{210}\text{Po}$ ), two  $\beta$ -sources ( $^{31}\text{Si}$  and  $^{42}\text{K}$ ) and a  $\gamma$ -source ( $^{241}\text{Am}$ ), see table I. For each source, the bias current was ramped close to the critical current while detection count rates were recorded, with the process repeated over hours of measurement.

Figure 2 shows  $\alpha$ -particle detection rates versus time for a given current bias. The  $^{210}\text{Po}$  source was mounted on a metallic holder on top of the detector to prevent detection of scintillation events from organic materials. The inset shows a simplified decay scheme for  $^{210}\text{Po}$ : an  $\alpha$ -emitting radionuclide which is rarely (0.0012 % probability) accompanied by  $\gamma$ -ray emission. The  $^{210}\text{Po}$  source had an activity of 41.4 kBq measured with a scintillation counter with an average  $\alpha$ -particle energy of 5.3 MeV and a half-life of  $t_{1/2} = 138.38$  days.<sup>13</sup> Because of the long half-life, we do not observe a decrease in the count rate over our limited measurement time; instead we observe a constant count rate with an average of  $582 \pm 43$  cps as shown in figure 2. In this arrangement the detector constituted a fraction  $\eta_d$  of the isotropic radiation sphere given by  $A/4\pi R^2$ , where  $A$  is the

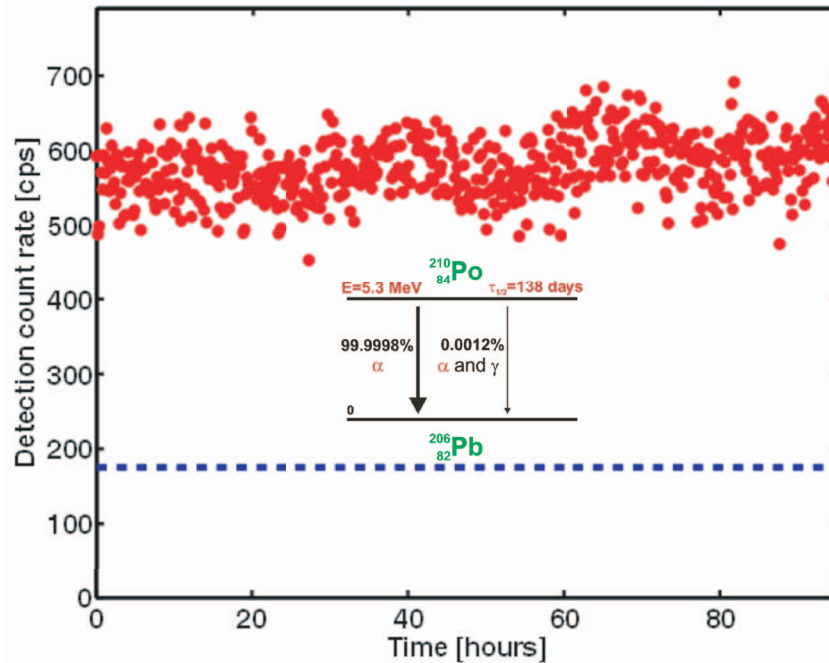


FIG. 2.  $\alpha$ -particle detection. Detection count rates recorded at  $I_b/I_c \sim 0.91$  for the  $^{210}\text{Po}$  source (red circles) and background counts (dashed blue line). The average count rate for the source is  $582 \pm 48$  cps and  $175 \pm 26$  cps for the background. A simplified decay scheme for  $^{210}\text{Po}$  is shown as an inset with  $^{210}\text{Po}$  decaying 99.9998% of the time with an  $\alpha$ -particle emission only.

active area of the SNPD, and  $R$  the source to detector distance. We have measured the detection efficiency  $DE = n_d/n_{\alpha p}$  where  $n_d$  is the detection rate and  $n_{\alpha p}$  is the estimated number of impinging alpha particles.  $n_{\alpha p}$  was measured as  $\eta_d \cdot A_0$ , where  $A_0$  is the initial source intensity measured with a scintillation counter. For an estimated distance of  $R \sim 25 \mu\text{m}$  (see Supplemental Material for Mounting<sup>12</sup>) and a source intensity of  $A_0 \sim 41 \text{ kBq}$ , the detection efficiency of the SNPD is  $\sim 78 \pm 18\%$  ( $407 \pm 55$  cps corrected for background counts). Since an  $\alpha$ -particle is a relatively massive particle, it could damage the NbTiN active layer.<sup>14</sup> With over  $1.7 \cdot 10^8$  detection events occurring during the 95 hours measurement with the  $\alpha$ -source, the detector revealed no decrease in the count rate, no increase in noise level and no modification of the critical current; thereby demonstrating radiation hardness.

To demonstrate  $\beta$ -particle detection, two different sources were used:  $^{42}\text{K}$  ( $t_{1/2} = 12.36$  hours) and  $^{31}\text{Si}$  ( $t_{1/2} = 2.62$  hours); see figure 3 insets for simplified decay schemes (For sample preparation see Supplemental Material<sup>12</sup>). It is important to note the  $\gamma$ -ray emission probabilities for each of these decays: while  $^{42}\text{K}$  is accompanied 17.64% of the time by a 1.524 MeV  $\gamma$ -ray,  $^{31}\text{Si}$  is a relatively pure  $\beta$ -emitting source.<sup>13</sup> Figure 3(a) shows the detection events from the  $^{42}\text{K}$  source measured over 26 hours. The half-life value extracted from the measurements is  $12.4 \pm 3.4$  hours. The detector noise floor is indicated by the dashed blue line. Following the same procedure for the shorter lived  $^{31}\text{Si}$  source, the exponential decay in figure 3(b) gives a half-life of  $2.9 \pm 0.5$  hours. Both  $^{42}\text{K}$  and  $^{31}\text{Si}$  half-life measured values are in good agreement with published data<sup>13</sup> and demonstrate single  $\beta$ -particle detection. The sources were mounted with a similar arrangement as for the  $^{210}\text{Po}$ . The distance  $R$  from source to detector was set to 1 mm for  $^{42}\text{K}$  and 2 mm for  $^{31}\text{Si}$  (see Supplemental Material for Mounting<sup>12</sup>). This combined with the initial activities of each source (see Table I) gives a detection efficiency of  $95 \pm 14\%$  and  $106 \pm 12\%$  for  $^{42}\text{K}$  and  $^{31}\text{Si}$ , respectively.

A measurement was carried out to determine the sensitivity of the detector towards  $\gamma$ -rays. Since  $\alpha$ -particles are much easier to block than  $\beta$ -particles, an  $^{241}\text{Am}$  source was chosen for a test measurement.  $^{241}\text{Am}$  is an  $\alpha$ -emitting radionuclide whose decay is accompanied by significant

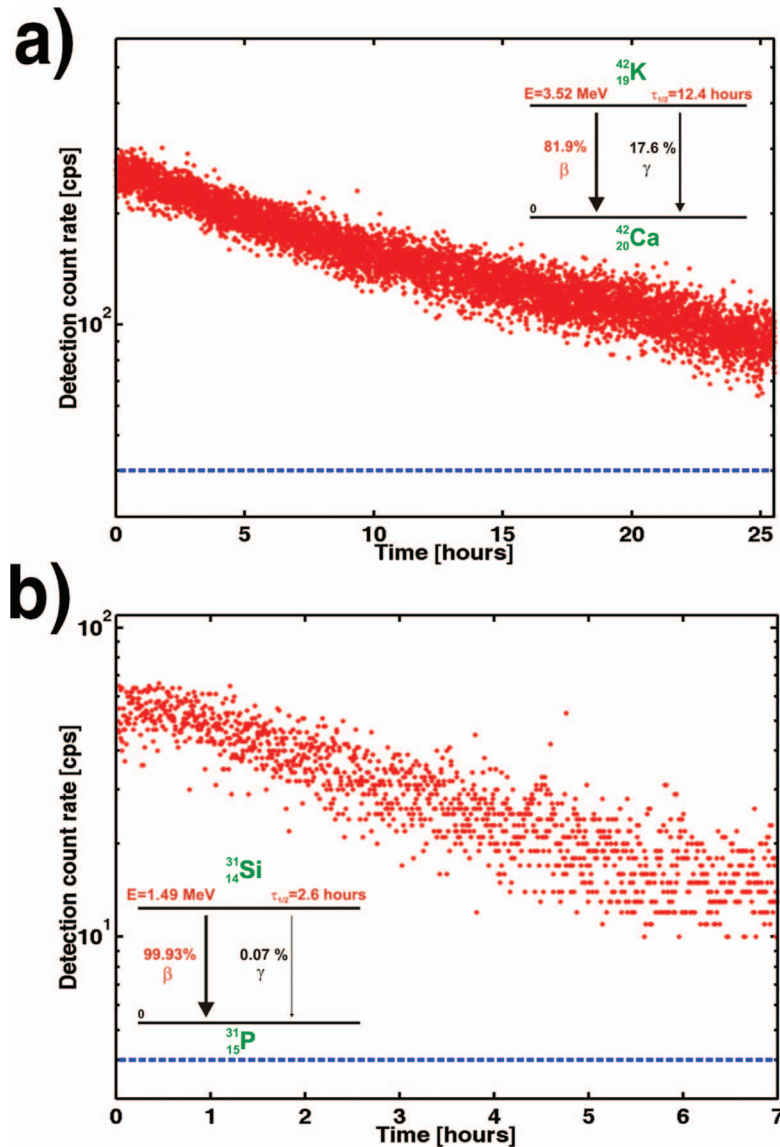


FIG. 3.  $\beta$ -particle detection. a)  $\beta$ -particle detection count rates measured with a  $^{42}\text{K}$  source. Detection count rates recorded at  $I_b/I_c \sim 0.95$  are shown as a semi-logarithmic plot versus time (red dots). b)  $\beta$ -particle detection count rates measured with a  $^{31}\text{Si}$  source. Detection count rates recorded at  $I_b/I_c \sim 0.88$  are shown as a semi-logarithmic plot versus time (red dots). The detector background level is indicated by the dashed blue line. A simplified decay scheme for both isotopes is shown as an inset.

amounts of other events (e.g. conversion and Auger electrons and X- and  $\gamma$ -ray emissions). We counted an electroplated  $^{241}\text{Am}$  source (a legacy source previously removed from a smoke detector) at approximately the same geometry as the  $^{210}\text{Po}$  source. This source was soldered to a threaded rod which helped to ensure a reproducible geometry. The measured count rate for the bare  $^{241}\text{Am}$  was  $5.75 \pm 0.43$  kcps and the dark count level (without the  $^{241}\text{Am}$  source) was measured to be  $2.07 \pm 0.20$  kcps. In order to measure only the  $\gamma$ -ray contribution to the count rate, we introduced a shield to block the  $\alpha$ -particles (and the conversion and Auger electrons) from reaching the detector. A small piece of aluminium foil ( $\sim 0.2$  mm thick) was used to cover the surface of the source. The count rate was then recorded for the shielded  $^{241}\text{Am}$  to check for  $\gamma$ -ray detection. The detection count rates dropped down to the dark count level, indicating that no X- nor  $\gamma$ -rays are detected. Table I presents

the detection efficiency of our superconducting nanowire detector for single particles ranging from single photons at optical frequencies to  $\alpha$ - and  $\beta$ -particles in the MeV range.

We have demonstrated an efficient nanoscale detector for single  $\alpha$ - and  $\beta$ -particles. The detection efficiency is close to unity for both particles. We note that no radiation damage was observed for our detector following more than 4 days of  $\alpha$ -particle irradiation, demonstrating the robustness of the detector. Furthermore, the nanoscaled detector exhibits blindness to  $\gamma$ - and X-rays. The increasing demands for radiation particle detector insensitive to saturating  $\gamma$ - or X-rays,<sup>15</sup> makes our detector a good candidate as a  $\gamma$ -discriminating detector. The detector could be mounted on a scanning probe to obtain spatially resolved particle detection measurements with unprecedented spatial resolution. Merging nanoscale detectors and particle detection is bound to enable a wide range of new applications where the high time, spatial resolution and high count rates will be essential.

## ACKNOWLEDGMENT

The authors thank Raymond N. Schouten for assistance with the electronics and T. Zijlstra for depositing the NbTiN layer. This work is supported financially by the Swedish Foundation for International Cooperation in Research and Higher Education (STINT) and by the Netherlands Organisation for Scientific Research (NWO/FOM) as well as SOLID (EU).

- <sup>1</sup> Becquerel, H., "Sur les radiations émises par phosphorescence," *Comptes Rendus*. **122**, 420–421 (1896).
- <sup>2</sup> Knoll, G. F., *Radiation Detection and Measurement* (John Wiley & Sons, Hoboken, 2010).
- <sup>3</sup> Pringle, R. W., *Nature* **166**, 11–14 (1950).
- <sup>4</sup> Hollander, J. M. and Perlman, I., *Science* **154**, 84–93 (1966).
- <sup>5</sup> Doriese, W. B., Ullom, J. N., Beall, J. A., Duncan, W. D., Ferreira, L., Hilton, G. C., Horansky, R. D., Irwin, K. D., Mates, J. A. B., Reintsema, C. D., Vale, L. R., Xu, Y., Zink, B. L., Rabin, M. W., Hoover, A. S., Rudy, C. R., and Vo, D. T., *Appl. Phys. Lett.* **90**, 193508 (2007).
- <sup>6</sup> Rabin, M. M., Hoover, A. S., Rudy, C. R., Lamont, S. P., Tournear, D. M., Vo, D. T., Beall, J. A., Doriese, W. B., Duncan, W. D., Ferreira, L., Hilton, G. C., Horansky, R. D., Irwin, K. D., O'Neil, G. C., Reintsema, C. D., Ullom, J. N., Vale, L. R., Chesson, K., and Zink, B. L., in *Microcalorimeter Nuclear Spectrometers: Proceedings of the 2006 IEEE Nuclear Science Symposium Conference Record*, IEEE Xplore. 544–547 (2006).
- <sup>7</sup> G. Gol'tsman, O. Okunev, G. Chulkova, A. Lipatov, A. Semenov, K. Smirnov, B. Voronov, A. Dzardanov, C. Williams, and R. Sobolewski, *Applied Physics Letters* **79**, 705 (2001).
- <sup>8</sup> Rosticher, M., Ladan, F. R., Maneval, J. P., Dorenbos, S. N., Zijlstra, T., Klapwijk, T. M., Zwiller, V., Lupascu, A., and Nogues, G., *Appl. Phys. Lett.* **97**, 183106 (2010).
- <sup>9</sup> S. Dorenbos, E. Reiger, U. Perinetti, V. Zwiller, T. Zijlstra, and T. Klapwijk, *Applied Physics Letters* **93**, 131101 (2008).
- <sup>10</sup> A. Semenov, G. Gol'tsman, and A. Korneev, *Physica C: Superconductivity* **351**, 349 (2001).
- <sup>11</sup> M. Tanner, C. Natarajan, V. Pottapenjara, J. O'Connor, R. Warburton, R. Hadfield, B. Baek, S. Nam, S. N. Dorenbos, E. Ureña, T. Zijlstra, T. Klapwijk, and V. Zwiller, *Applied Physics Letters* **96**, 221109 (2010).
- <sup>12</sup> See supplementary material at <http://dx.doi.org/10.1063/1.4740074> for sample preparation, mounting and electrical readout.
- <sup>13</sup> Firestone, R. B., and Shirley, V. S., *Table of Isotopes* (eighth ed. Wiley, New York, 1996).
- <sup>14</sup> Lindström, G., and Fretwurst, M. M. E., *Nucl. Inst. Methods Phys. Res A* **426**, 1–15 (1999).
- <sup>15</sup> Martoff, C. J., *Science* **237**, 507–509 (1987).